

# Improved structural ordering in sexithiophene thick films grown on single crystal oxide substrates

C. Aruta\*, P. D'Angelo, M. Barra, G. Ausanio and A. Cassinese

*CNR-INFM Coherentia and Dipartimento di Scienze Fisiche,*

*Università di Napoli "Federico II",*

*Piazzale Tecchio 80, Napoli 80125, Italy*

(Dated: February 5, 2020)

## Abstract

We report on sexithiophene films, about 150nm thick, grown by thermal evaporation on single crystal oxides and, as comparison, on  $Si/SiO_2$ . By heating the entire deposition chamber at  $100^\circ C$  we obtain standing-up oriented molecules all over the bulk thickness. Surface morphology shows step-like islands, each step being only one monolayer height. The constant and uniform warming of the molecules obtained by heating the entire deposition chamber allows a stable diffusion-limited growth process. Therefore, the regular growth kinetic is preserved when increasing the thickness of the film. Electrical measurements on differently structured films evidence the impact of the inter island separation region size on the main charge transport parameters.

PACS numbers: 81.10.Aj; 61.66.Hq; 85.30.Tv

---

\* Correspondence should be addressed to: [carmela.aruta@na.infn.it](mailto:carmela.aruta@na.infn.it)

## I. INTRODUCTION

The increasing attention towards organic electronics has been requiring a deeper knowledge of the materials and interfaces affecting electrical transport properties in organic films [1]. Understanding the relationship between film morphology and charge transport is a key issue to improve the devices performances. In particular, the substrate surface and the growth conditions have shown a strong influence on the structural and electronic properties of organic films[2, 3]. Indeed, the film morphology at the buried interfaces can be different from that in the bulk [4], thus strongly affecting the charge transport in thin film transistors. Under this respect, anisotropic linear  $\pi$ -conjugated molecules like sexithiophene (T6) can be obtained as polycrystalline or highly oriented thin films [5, 6], with charge transport depending on the long range molecular ordering [7]. Because of electronic interactions between the molecules and active surfaces,  $\pi$ -conjugated molecules tend to grow in lying-mode on relatively active surfaces such as metals [8, 9, 10]. On the contrary, on relatively inert surfaces, such as  $SiO_2$  or  $KBr$  substrates [11, 12], these molecules can grow in the standing-mode. Lattice incommensurability or roughness of the substrates also influence the growth mode of  $\pi$ -conjugated molecules. Standing mode or flat-lying-mode growth is observed on poly-crystalline [13] or single-crystalline metal surfaces [9, 14], respectively. In addition, nucleation and growth processes strongly influence the structure and morphology of high-vacuum evaporated long-chain molecules[15]. In thick films (thickness higher than 100nm) the three-dimensional (3D) growth maintains a memory of a layer-by-layer growth, even after the first nucleation process is completed[16]. Therefore, both layer-plus-island (Stranski-Krastanov) and island (Vollmer-Weber) growth modes can be observed. The size of the 3D-grains was shown to increase upon using increased substrate temperatures, indicating that the growth mode is a diffusion-limited process[16, 17]. Well-defined structural properties are crucial both for fundamental studies and for fabrication of optimal devices, but the control of the growth of thick films can be further improved. In this work we report on highly structured thick T6 films (about 150nm thick) grown by heating the entire deposition chamber. Like that, both standing and lying molecules are equally warmed, in spite of their different surface-area/volume ratio and the growth temperature have the same effect on the growth kinetic of both types of molecular orientation. Hundreds nanometers thick films are particularly important in view of possible

applications, such as organic spin-valves or Field Effect Transistors (FET) with a vertical structure, where different substrates are also employed. We have grown T6 films on the single crystal substrates,  $Al_2O_3$  (sapphire) r-plane and MgO (100). Both substrates have similar physical properties, such as for example the dielectric constant (about 10) and the thermal conductivity (about  $30 W/mK$ ). Quite the reverse, the in-plane lattice structures are different:  $Al_2O_3$  r-plane has the in-plane hexagonal lattice with both  $a$  and  $b$  axes equal to  $4.75\text{\AA}$ , while  $MgO$  (100) has the in-plane square lattice with axis  $4.21\text{\AA}$ . Nevertheless, we find similar structural, morphological and electrical properties in T6 films grown on both substrates. Although, there has been a considerable effort towards the control of T6 growth when in form of very thin films, the study of thicker films on oxide substrate can be further refined[18]. The results on single crystal oxides are compared with films grown during the same deposition process on  $Si/SiO_2(100)$ , the typical substrate used for electrical properties and growth processes investigation.

## II. EXPERIMENTAL

T6 films were vacuum evaporated by a Knudsen cell with a base pressure of  $1-3 \times 10^{-7}$  mbar. The deposition rate and the thickness were monitored by a quartz oscillator, with averaged growth rate ranging between  $0.2$  and  $0.4\text{\AA}/\text{sec}$ . The film thickness was also controlled by a TENCOR profilometer. The sample holder allowed the simultaneous growth of two  $10 \times 10\text{mm}^2$  films. For the optimization of T6 films, we used a peculiar sample heating procedure, consisting in keeping warm the entire chamber at the same temperature of  $100^\circ\text{C}$  for 24 hours, before to proceed with the deposition. Such expedient allows a warm environment which favors the heating of both sides of the samples. All films were structurally and morphologically characterized. Because of the heavy sulphur atoms in the T6 structure, it is possible to get important information on the structural properties by X-ray diffraction (XRD) with a conventional X-ray source. We used the Bragg-Brentano geometry in symmetrical reflection mode, the Cu  $K\alpha$  wavelength and a graphite monochromator. In addition, an Atomic Force Microscopy (AFM) (Digital Instruments Nanoscope IIIa), equipped with a sharpened silicon tip with an apical curvature radius  $\leq 5\text{nm}$ , was used in tapping mode with a rate of 1Hz, to obtain images of the surface profile under ambient conditions. After min-

imizing the tip size effect by the deconvolution on each AFM image, the three-dimensional view of the deposits was reconstructed. The electrical properties have been also investigated by Current-Voltage (I-V) measurements. All measurements were performed on planar samples, in vacuum ( $10^{-3}$  mbar), by means of a Keithley 487 picoammeter. A standard two probe technique was employed by a cryogenic probe station. In plane silver contacts have been grown on the surface film (top contacts), obtaining conducting channels with length  $L = 100\mu m$  and width  $w = 5mm$ . Finally, FET devices have been fabricated by depositing T6 films on  $SiO_2$  200nm thick, thermally grown on heavily n-doped Si gate electrode, with interdigitated gold source and drain contacts (bottom contact). These electrodes provide a channel length  $L = 40\mu m$  and a channel width  $w = 20mm$ .

### III. RESULTS AND DISCUSSION

A typical XRD spectrum of the optimized T6 film grown on  $Al_2O_3$  substrate is reported in fig.1(a). We can index the reflections by using the low-temperature single crystal data. Such a structure corresponds to the  $P2_1/n$  space group with  $a = 44.708\text{\AA}$ ,  $b = 7.851\text{\AA}$  and  $c = 6.029\text{\AA}$ [19]. Only the  $(h00)$  reflections of the T6 compound can be observed. Therefore, T6 films on single crystal oxides result very well aligned with the long axis along the direction perpendicular to the substrate surface. The noticeable result is the presence of high order reflections up to  $(34,0,0)$  and the very narrow rocking curve of the high-order reflection  $(20,0,0)$  reported in fig.1(b), with a Full Width at Half Maximum (FWHM) about  $0.2^\circ$ . Typical values of the rocking curve, which are considered extremely low for an organic film, are of the order of  $1^\circ$ [20], though the measurements were performed by synchrotron radiation on lower order reflections. Our structural data demonstrate the improved crystal quality of T6 films grown in a warmed environment, being the structural ordering propagated along the whole 150nm thickness. The corresponding AFM images are reported in fig.2. Domains of about one micron large can be observed in fig.2(a), which are composed by step-like circular aggregates. The cross-section reported in fig.2(c) of the smaller AFM scan size of fig.2(b) reveals that the step height is about one molecule. Together with the XRD results, we can infer that each terrace is very well structured, with molecules vertically arranged. XRD data of T6 films grown on  $Si/SiO_2$  substrate reported in fig. 3(a) show that the molecules prevalently orient with the long axis perpendicular to the substrate surface also

on  $Si/SiO_2$ , in agreement with the results reported in literature[6]. However, in such a case we can detect minor order reflections in the  $\Theta - 2\Theta$  spectra [fig. 3(a)], up to the (22,0,0) only. The FWHM of the rocking curve of the (20,0,0) T6 peak reported in fig. 3 (b) is about  $0.5^\circ$ . The presence of minor order reflections and the larger rocking curve in the case of  $Si/SiO_2$  with respect to the  $Al_2O_3$  substrate, reveal the minor crystal quality of T6 films on  $Si/SiO_2$ . It has been reported that molecules perpendicular and parallel to the substrate can be simultaneously present in T6 films with submonolayer coverage grown on silicon dioxide[21]. Such an interface disorder will prevent the growth of a well ordered T6 film, in agreement with our findings. XRD results are confirmed by the AFM measurements reported in fig.4, which reveal smaller size domains with a non homogeneous distribution in case of T6 films on  $Si/SiO_2$ . Regular step-like islands are occasionally observed [fig. 4(b)]. On the contrary, we find high crystal quality and equivalent morphology in both  $Al_2O_3$  and  $MgO$  single crystal oxides. We can tentatively ascribe the good crystal quality of our thick films grown at  $100^\circ C$  to the uniform growth temperature of the whole film thickness. Indeed, by heating all the chamber, the surface of the film is always at the same temperature during the growth process. On the contrary, in case of conventional heating of the film from the back of the substrate, the heat transfer changes by increasing the film thickness and the surface of the growing film could not be at the ideal temperature during all the deposition process[22]. It has been reported that islands made of standing molecules can progressively incorporate flat-lying molecules during the evolution of the growth process [23]. The appearance of standing molecules in thick films is suggested to be a result of a gradual deterioration of the ordering of the lying molecules occurred during the increasing of the film thickness[24]. On the contrary, our structural and morphological data show that the bulk of the film is formed by ordered vertical standing molecules. However, Kowarik *et al.* [25] found that, as a general feature of the growth of organics, the molecules prefer the lying-down orientation when the van der Waals interaction on the stepped sapphire surface is important. In our case, the uniform heating by the warmed chamber increases the mobility of the molecules, favoring the standing-up orientation. Theoretical calculations of Kubono *et al.*[26] demonstrates that standing molecules increase faster than lying molecules when the substrate temperature is higher. Therefore, we can guess that the uniform heating further increases this effect. Indeed, the growth temperature have the same effect on the growth kinetic of both standing and lying molecules which are equally warmed, in spite of

their different surface-area/volume ratio. As a matter of fact, the lattice match is not the principal factor governing the organic mechanism of growth. A further evidence of this aspect is given by the employment of different single crystal substrates, such as  $MgO$ , which give also rise to well oriented molecules. The differences between the single crystal oxides and the  $Si/SiO_2$  substrates can be related to the different surface chemical composition[23] and/or surface crystal order[24], thus changing the surface energy. The growth process is controlled not only by the chemical interaction between the molecule and the substrate surface [16] but also by the kinetics mediated by the substrate surface order, with the latter dominating in weakly interacting systems[24]. The silicon oxide layer on our  $Si/SiO_2$  substrates is not well structured, as confirmed by the absence of any silicon oxide reflection by XRD and a smoother substrate surface by AFM. On the contrary,  $Al_2O_3$  substrates have edges along the crystal directions which act as nucleation centers. It is well established that, because of the strong electrostatic field at step edges, isolated molecules absorb preferentially there.

In order to complete our study, the electrical properties of the T6 films have been investigated both by bulk I-V measurements and FET techniques. In any case, the measurements have been performed in darkness and in vacuum (typically  $10^{-3}$  mbar) to strongly reduce the effects of ambient doping (i.e.  $O_2$  and  $H_2O$ ). Bulk I-V measurements have been carried out only in the case of T6 films deposited on single crystal oxide substrates, since undesired leakage currents were observed at high fields on  $Si/SiO_2$  substrates. For all investigated samples, at low voltages ( $V < 100Volt$ ,  $E < 10^4V/cm$ ) I-V curves show a linear behavior according to the basic Ohm's law. Conductivity values extracted in this current range showed to be strongly affected by the film morphology, as demonstrated by the comparison between I-V curves for films grown in the warmed chamber and at  $100^\circ C$  (fig.5). Indeed, the XRD spectra of the two films (inset of fig.5) reveal an appreciable improvement in the case of films grown in the warmed chamber. Furthermore, in T6 films grown at room temperature, few grains differently oriented are also present, as confirmed by the detection of other reflections different from the  $(h00)s$  in the XRD spectra. Anyway, I-V measurements in fig.5 show that, despite the worst structural organization, the conductivity values (from  $5 \cdot 10^{-8}S/cm$  to  $6 \cdot 10^{-7}S/cm$ ) of films deposited at room temperature are higher than those extracted for films grown at  $100^\circ C$  (between  $5 \cdot 10^{-9}S/cm$  and  $3 \cdot 10^{-8}S/cm$ ). At higher voltages, all bulk I-V measurements follow a super-linear trend which can be well fitted by a square power law. By assuming that in this range the current is limited by space charge

effects (Space Charge Limited Current regime) in presence of uniformly distributed traps [31], the I-V characteristics can be modelled by a basic formula valid for in-plane transport measurements[32]:

$$I = \left( \frac{2}{\pi} w \cdot \mu_B \cdot \epsilon_0 \cdot \epsilon_r \cdot \frac{V^2}{L^2} \right)$$

where  $\epsilon_r$  is the T6 dielectric permittivity (about 3) and  $\mu_B$  is the bulk mobility related to the free carries in the whole film. By using this formula to fit the experimental measurements, we have obtained that room temperature bulk mobility  $\mu_B$  of the charge carriers, down-scaled by the ratio between free and trapped carriers [30], ranges between  $5 \cdot 10^{-5}$  and  $1 \cdot 10^{-4} cm^2/Volt \cdot sec$  for T6 films grown in warmed environment. In the same way,  $\mu_B$  has been estimated to be about  $5 \cdot 10^{-2} cm^2/Volt \cdot sec$  for films grown at room temperature. The better I-V performances of the films grown at room temperature, seem to suggest that the packed structure related to the small grain morphology better supports the charge carrier bulk transport, if compared to the step-islands morphology, where the presence of large boundary regions can reduce the occurrence of conduction percolating paths[29].

I-V curves measured at different temperatures for a T6 film deposited on  $Al_2O_3$  in warmed environment are reported in Fig.6. It is worth to mention that both bulk mobility and conductivity extracted by I-V curves obey a standard Arrhenius law (inset of fig.6) with an activation energy  $\Delta_B$  very close to 0.2 eV in the range between 295 K and 335 K.

FET measurements have been performed on T6 films with thickness ranging between 20 nm ad 150 nm grown both in warmed and room temperature environment. In any case, the responses of our T6 transistors exhibit some typical features of the electrical transport regimes dominated by charge carriers trapping phenomena[27, 28]. As shown in fig.7, where the output characteristics,  $I_{DS}$  vs  $V_{DS}$  (drain-source current versus voltage) curves at fixed  $V_G$  (gate voltage) of a T6 FET device grown in warmed environment are reported, the currents slightly decay in the heart of the saturation region ( $V_G \sim V_{DS}$ )[27]. Similarly, the trapping effects provide the hysteresis in the measured transfer curves ( $I_{DS} - V_G$  at fixed  $V_{DS} = -5Volt$ ) where (see inset of fig.7) the current in the direct gate voltage scan from +20 (off state) to -50 V (on state) is always higher than that of the inverse scan (from -50 to +20 V, where the device turns off). In this work, the mobility of free charge carriers ( $\mu_{FET}$ ) has been simply evaluated by the slope of the direct scan of the transfer curve in the linear regime ( $V_G \gg V_{DS}$ ), according to the basic formula:

$$g_m = \frac{\partial I_{DS}}{\partial V_G} = \frac{wC_i\mu_{FET}}{L}$$

where  $C_i$  (about  $17nF/cm^2$ ) is the insulator capacitance per unit area. Following this procedure,  $\mu_{FET}$  values between 1.1 and  $1.5 \cdot 10^{-2} cm^2/Volt \cdot sec$  have been typically estimated at room temperature for T6 films grown in warm environment. No clear thickness dependence of mobility has been evidenced in our study, supporting the basic vision that the field effect involves only a few nanometers thick region at the interface between dielectric and organic film. These results and the extracted mobility values are in good agreement with previous reports[33]. On the contrary, for T6 films grown in room temperature environment,  $\mu_{FET}$  always resulted lower than  $1 \cdot 10^{-3} cm^2/Volt \cdot sec$  and with less reproducibility among the different samples. Finally, also for T6 measurements, we found that mobility is thermally activated, with typical activation energies  $\Delta_{FET}$  between 60 and 90 meV. The large discrepancy between the electrical behavior and the related physical parameters checked in bulk and FET measurements are necessarily due to different electron transport phenomena involved, which primarily reflect the different energy state density affecting the charge carriers motion occurring in bulk and interface regions[34]. Furthermore, as stated above, I-V and FET measurements are performed on films grown on different substrates and with slightly different morphologies. In order to better address these fundamental issues, further studies, on both field effect and vertical devices of T6 films grown on single crystal oxides, are envisaged.

#### IV. CONCLUSIONS

We have shown that T6 thick films grown on single crystal oxides by heating the whole chamber at  $100^\circ C$ , have a noticeable good crystal quality all over the thickness of about 150nm. We can explain such a result in terms of surface temperature of the film which is constant during the whole process and uniform along the whole molecule, thus favoring standing-up orientation. At our growth conditions, the localized substrate/molecule interactions occurring in the early growth stages determine the crystal quality of the whole film, even in the case of such sizeable thickness. Indeed, minor crystal quality is obtained for T6 films on  $Si/SiO_2$  substrate. Such a difference respect to the single crystal oxide substrates



can be associated to the surface crystal ordering. Density of nuclei depends upon the nature of the substrate and affects the earlier stage of growth when 3D-islands start to form. In particular, step-edges at the single-crystal oxide surfaces act as stable anchoring sites for the molecules. Successively, other arriving molecules diffuse on the surface until they anchor to the previous ones. Such a diffusion-controlled growth depends on the mobility of molecules and it is favored by the uniform and constant growth temperature we used. The grain boundaries between large step-like islands with well oriented molecules limit the long-range electrical in-plane transport, as demonstrated by our electrical measurements. However, well-defined anisotropic structural features are crucial for fundamental study of the anisotropic charge transport in such a long-chain  $\pi$ -conjugated molecules. The control of the growth process and the physical properties of thick films will be useful to better understand the role of the interface as well as of the bulk. This can be relevant for the design of devices based on vertical structure such as rectifying diodes and organic spin valves.

## V. ACKNOWLEDGMENTS

We acknowledge stimulating discussions with C. Albonetti, F. Biscarini and E. Lunedei. Fruitful discussions of the XRD data with A. Geddo-Lehmann are also acknowledged.

- 
- [1] C. Kim, A. Facchetti, T. J. Marks, *Science* **318**, 76 (2007)
- [2] D. Fichou *J. Mater. Chem.* **10**, 571 (2000)
- [3] X. J. Yu, J. B. Xu, W. Y. Cheung, N. Ke *J. Appl. Phys.* **102**, 103711 (2007)
- [4] R.J. Kline et al. *Nature* **5**, 222 (2006)
- [5] B. Servet, G. Horowitz, S. Ries, O. Lagorsse, P. Alnot, A. Yassar, F. Deloffre, P. Srivastava, R. Hajlaoui, P. Lang, F. Garnier, *Chem. Mater.* **6**, 1809 (1994)
- [6] J.Ivanco, J.R. Krenn, M.G. Ramsey, F.P. Netzer, T. Haber, R.Resel, A. Haase, B. Stadlober, G. Jakopic, *J. Appl. Phys.* **96**, 2716 (2004)
- [7] F. Garnier, G. Horowitz, D. Fichou and A. Yassar, *Supramol. Sci.*,**4**, 155 (1997)
- [8] S. Lukas, S. Sohnchen, G. Witte, C. Woll, *Chem. Phys. Chem.* **5**, 266(2004)
- [9] G. Yoshikawa, M. Kiguchi, S. Ikeda, K. Saiki, *Surf. Sci.* **559**, 77 (2004)
- [10] M. Kiguchi, G. Yoshikawa, K. Saiki, *J. Appl. Phys.* **94**, 4866 (2003)
- [11] K. Hamano, T. Kurata, S. Kubota, H. Koezuka, *Jpn. J. Appl. Phys.* **33**, L1031 (1994)
- [12] S. Ikeda, M. Kiguchi, Y. Yoshida, K. Yase, T. Mitsunaga, K. Inaba, K. Saiki, *J. Cryst. Growth* **265**, 296 (2004)
- [13] T. Okajima, S. Narioka, S. Tanimura, K. Hamano, T. Kurata, Y. Uehara, T. Araki, H. Ishii, Y. Ouchi, K. Seki, T. Ogama, H. Koezuka, *J. Electron Spectrosc.* **78**, 379 (1996)
- [14] M. Kiguchi, S. Entani, K. Saiki, G. Yoshikawa, *Appl. Phys. Lett.* **84**, 3444 (2004)
- [15] M. Muccini, M. Murgia, F. Biscarini, C. Taliani, *Adv. Mat.* **13**, 355 (2001)
- [16] F. Biscarini, R. Zamboni, P. Samori, P. Ostojca, C. Taliani, *Phys. Rev. B* **52**, 14868 (1995)
- [17] F. Biscarini, P. Samori, O. Greco and R. Zamboni, *Phys. Rev. Lett.* **78**, 2389 (1997)
- [18] S. Blumstengel, N. Koch, S. Sadofev, P. Schfer, H. Glowatzki, R. L. Johnson, J. P. Rabe, and F. Henneberger, *Appl. Phys. Lett.* **92**, 193303 (2008)
- [19] G. Horowitz, B. Bachet, A. Yassar, P. Lang, F. Demanze, J.L. Fave, and F. Garnier, *Chem. Mater.* **7**, 1337 (1995)
- [20] M. Oehzelt et al. *Adv. Mater.* **18**, 2466 (2006)
- [21] M. A. Loi, E. Da Como, F. Dinelli, M. Murgia, R. Zamboni, F. Biscarini, M. Muccini, *Nature Materials* **4**, 81 (2005)
- [22] A. Cassinese, M. Getta, M. Hein, T. Kaiser, H.G. Kurschner, B. Lehndorff, G. Muller, H.

- Piel, B. Skriba, IEEE Trans. on Appl. Sup.**9**, 1960 (1999)
- [23] F. Dinelli, J.-F. Moulin, M.A. Loi, E. Da Como, M. Massi, M. Murgia, M. Muccini, F. Biscarini, J. Wie, P. Kingshott, J. Phys. Chem. B **110**, 258 (2006)
- [24] J. Ivanco, T. Haber, J.R. Krenn, F.P. Netzer, R. Resel , M.G. Ramsey, Surf. Sci. **601**, 178 (2007)
- [25] S. Kowarik, A. Gerlach, S. Seller, F. Schreiber, L. Cavalcanti and O.Konovalov, Phys. Rev. Lett. **96**, 125505 (2006)
- [26] A. Kubono, R. Akiyama, Mol. Cryst. Liquid Cryst. **378**, 167 (2002)
- [27] P. Stallinga , H. L. Gomes , F. Biscarini, M. Murgia, D. M. de Leeuw, J. Appl. Phys **96**, 5277 (2004)
- [28] L. Torsi, A. Dodabalaphur, L. J. Rothberg, A. W. P. Fung, H. E. Katz, Phys. Rev. B. **57**, 2271 (1998)
- [29] S. Y. Yang, K. Shin, Se H. Kim, H. Jeon, J. Ho Kang, H. Yang and C. E. Park J. Phys. Chem. B **110**, 20302 (2006)
- [30] M. A. Lampert and P. Mark, Current injection in Solids, NY. Lond. (1970).
- [31] G. Horowitz, Adv. Mat. **10**, 365 (1998)
- [32] J.A. Geurst, Phys. Stat. Sol. **15**, 10 (1966)
- [33] Franco Dinelli, Mauro Murgia, Pablo Levy, Massimiliano Cavallini, Fabio Biscarini, and Dago M. de Leeuw Phys. Rev. Lett. **92**, 116802 (2004)
- [34] C. Tanase, E.J. Mejer , P.W.M. Blom, D.M. De Leeuw, Phys. Rev. Lett. **91**, 216601 (2003)

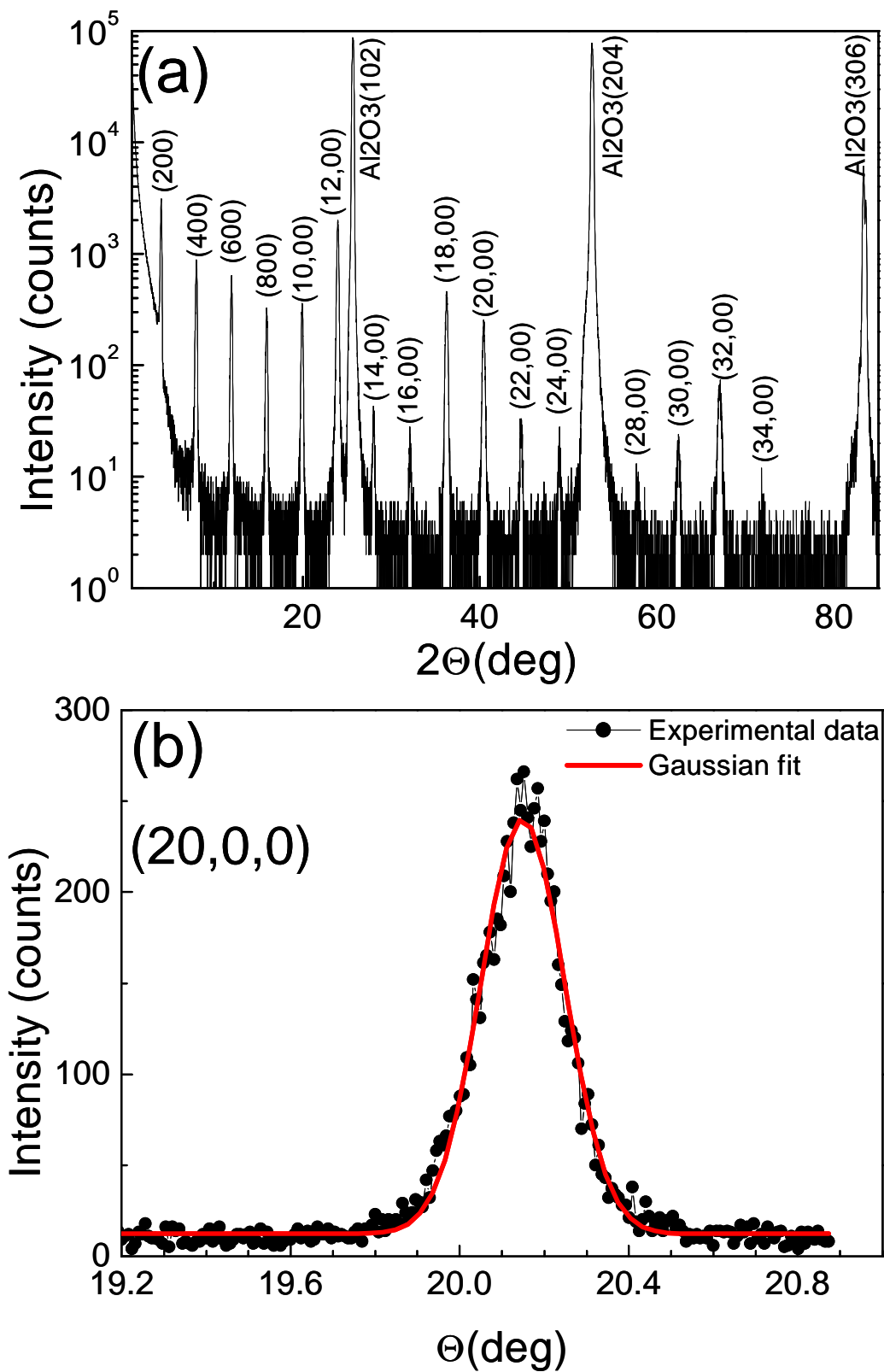


Figure 1: (Color online) (a) XRD measurements of an optimized T6 film grown at  $100^\circ C$  on  $Al_2O_3$  substrate. (b) Rocking curve of the (20,0,0) reflection.

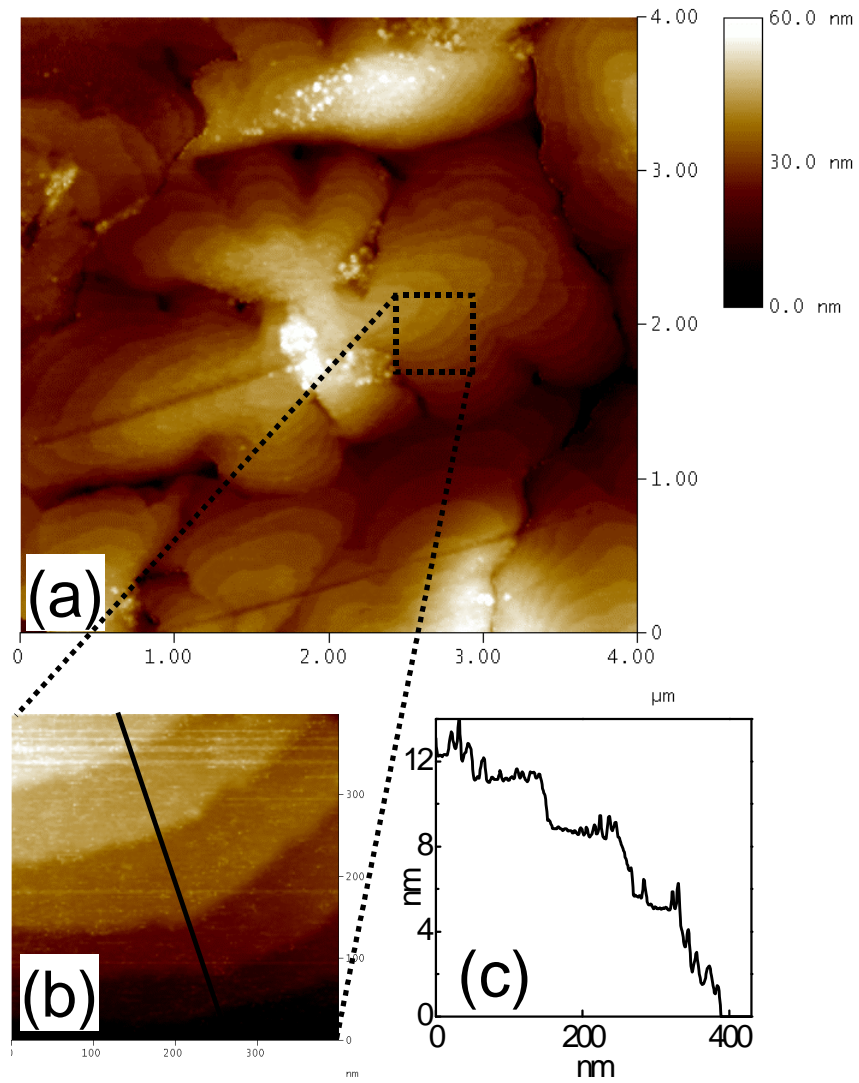


Figure 2: (Color online) AFM images of an optimized T6 film grown at  $100^{\circ}\text{C}$  on  $\text{Al}_2\text{O}_3$  substrate: (a) scan size of  $4 \times 4 \mu\text{m}$  and Z-range  $0 - 60 \text{ nm}$ , (b) scan size of  $430 \times 430 \text{ nm}$  and Z-range  $0 - 20 \text{ nm}$ , (c) cross section along the straight line of panel (b).

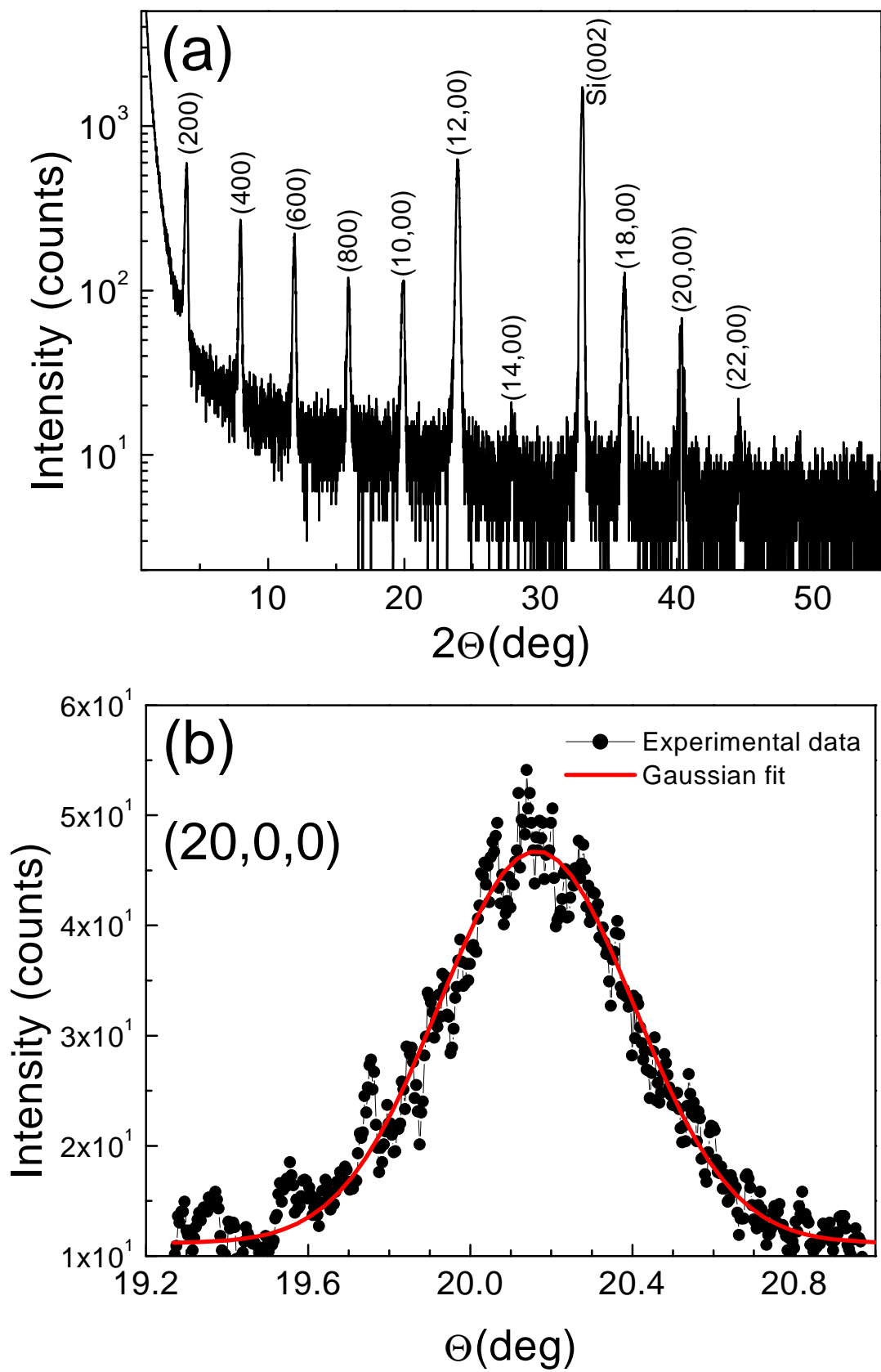


Figure 3: (Color online) (a) XRD measurements of a T6 film grown at  $100^\circ\text{C}$  on  $\text{Si}/\text{SiO}_2$  substrate. (b) Rocking curve of the (20,0,0) reflection.

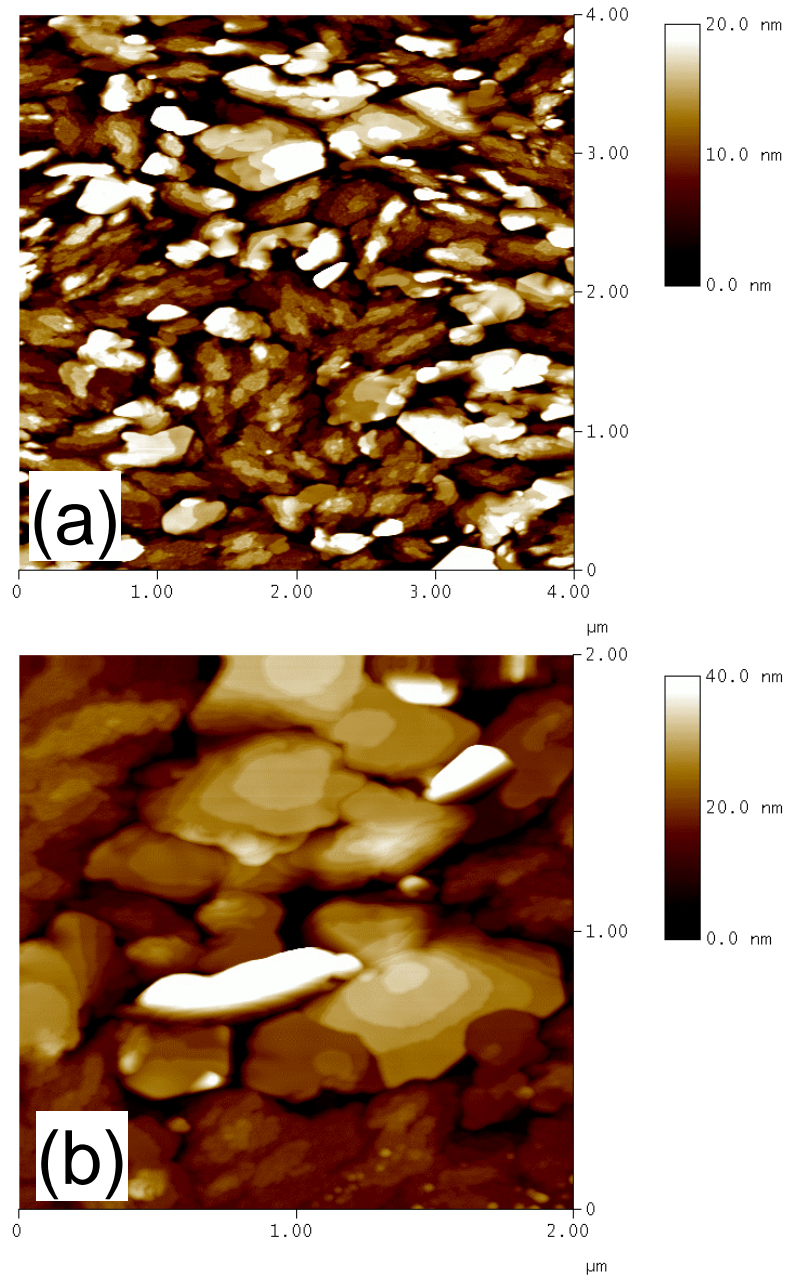


Figure 4: (Color online) AFM images of a T6 film grown at  $100^{\circ}\text{C}$  on  $\text{Si}/\text{SiO}_2$  substrate: (a) scan size of  $4 \times 4 \mu\text{m}$  and (b) scan size of  $2 \times 2 \mu\text{m}$ .

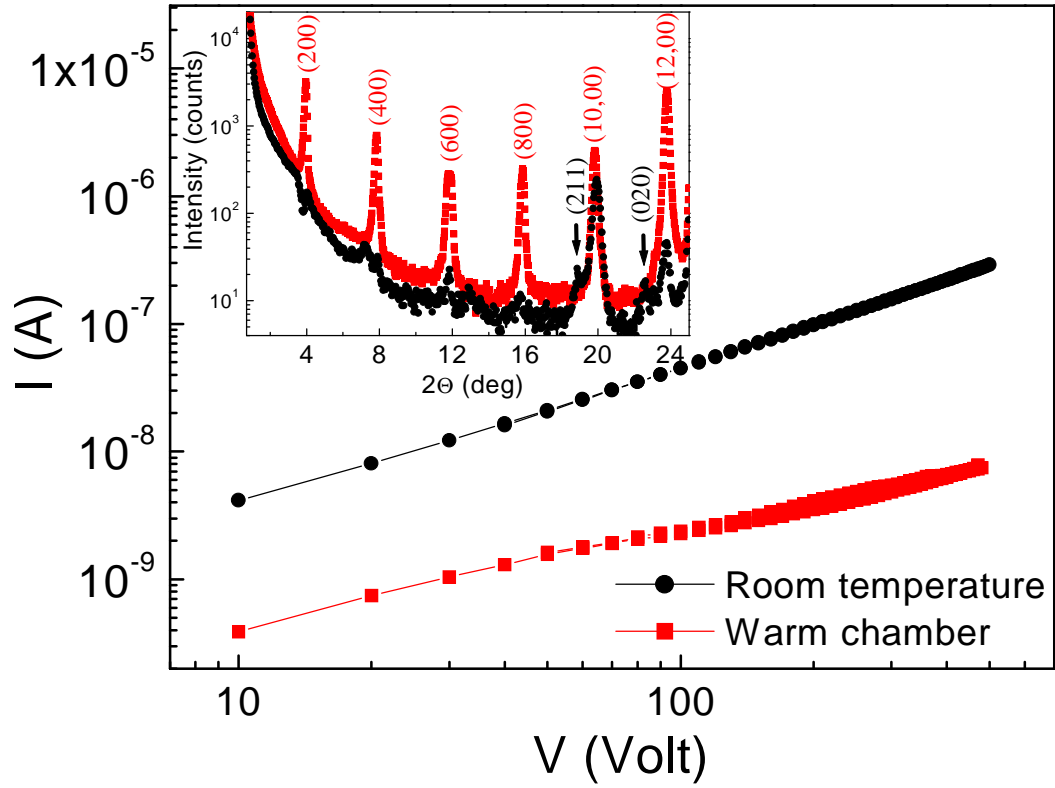


Figure 5: (Color online) Bulk I-V measurements of T6 films deposited at room temperature and in the warmed environment on  $Al_2O_3$  substrate. In the inset, the comparison of the corresponding XRD spectra is also reported.



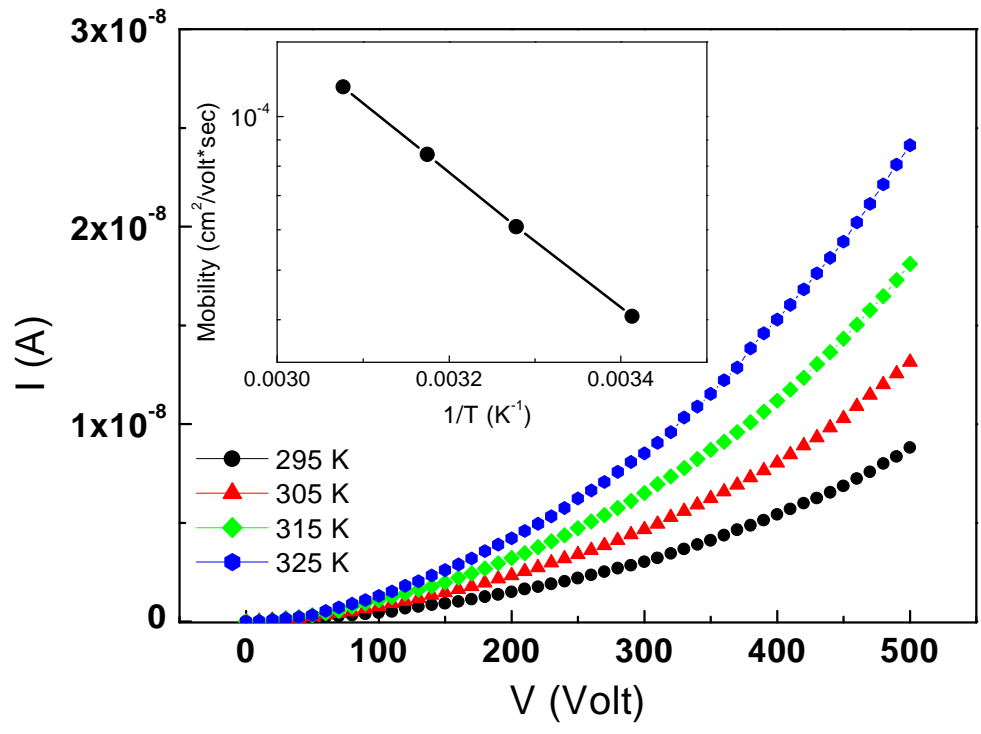


Figure 6: (Color online) Bulk I-V measurements at different temperatures for a T6 film deposited on  $Al_2O_3$  substrate. The mobility as a function of the inverse temperature is reported in the inset.

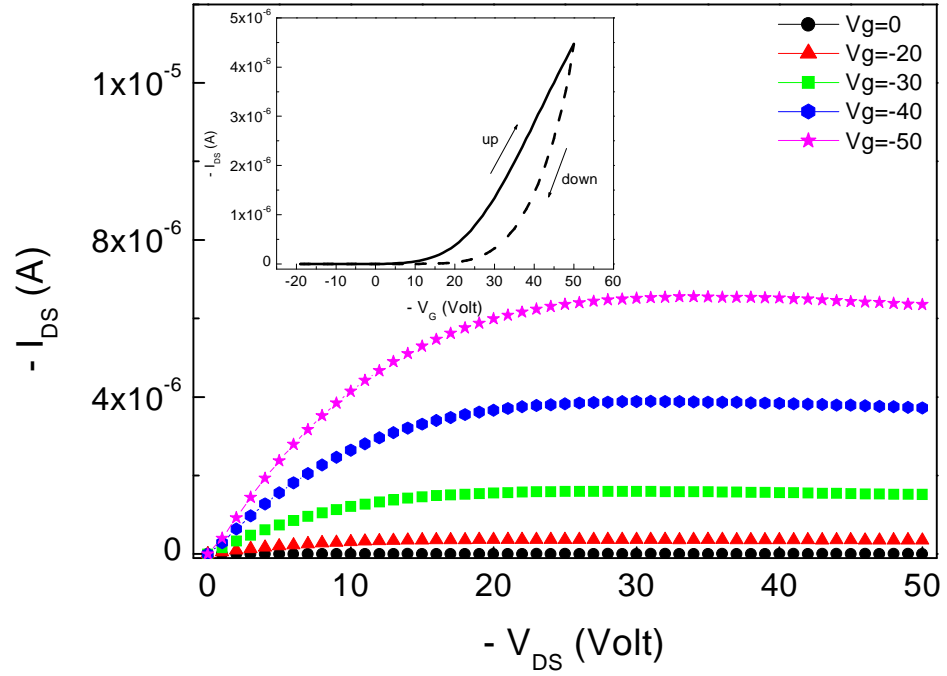


Figure 7: (Color online)  $I_{DS} - V_{DS}$  curves for a T6 FET device at various gate voltages ( $V_G$ ). In the inset the transfer curve measurement at  $V_{DS} = -5$  Volt is reported.